Conformations of Poly(diethylsiloxane) and Its Mesophase Transitions

Kenneth J. Miller, Janusz Grebowicz,† John P. Wesson,‡ and Bernhard Wunderlich*,§

Department of Chemistry, Rensselaer Polytechnic Institute, Troy, New York 12180-3590.
Received December 27, 1988; Revised Manuscript Received June 30, 1989

ABSTRACT: Molecular mechanics calculations on the isolated molecule are used in a discussion of the transitions of poly(diethylsiloxane) from the rigid crystal, α, to the condis crystal, β, at T_d, to another mesophase, α_m, at T_i, and finally to the isotropic melt at T_x. Ethyl groups in optimum orientations in the sequence O–Si–C are nearly trans (t) or gauche (g^+ and g^-). The trans and gauche conformations are separated by a small potential barrier. The four ethyl groups in a dimer yield conformations consisting of combinations of t, g^+, and g^-. Minimum energy conformations of the backbone chain dimers are found to be flat, f_1f_2, left- and right-handed helices, c_1c_2, bent conformations with a vertical plane of symmetry, v_1v_2, and asymmetric mixtures. Only the flat conformations fulfill the requirements of extended, straight-chain conformations for packing in the crystal. Two families of conformations occur: I with tttt, g^+ttt, and g^+tg^+t and II with $g^+tg^+g^-$ and $g^+g^-g^+g^-$ type ethyl groups. The volume and surface area increase with increasing number of gauche ethyl groups, and the average volume of family II is greater than that of family I by about 5% which correlates with the volume change from the α to the β phase. The α (α_1 and α_2) and β (β_1 and β_2) phases are thus rationalized by families I and II. The condis transition is attributed to increased mobility of the ethyl groups and a change from family I to family II. The α_m phase is discussed in terms of maximum mobility of the ethyl groups with increased numbers of different types of long-chain conformations still forcing segments of the chain to be straight by intramolecular interaction. Finally, in the melt helices with large turns and bends in the chain are possible, connected through transition regions.

Introduction

Mesophase materials can be classified as liquid crystals, plastic crystals, and condis crystals. Liquid crystals are positionally mobile and disordered, plastic crystals are orientationally mobile and disordered, and, analogous to the other two mesophases, condis crystals are *conformationally disordered.*[1] The condition for stability of a condis crystal is the existence of multiple conformational isomers of similar energy, so that cooperative motion between the different conformations does not destroy orientational and positional order in the crystal. In a recent review paper, we presented many examples of small molecules and polymers for which condis crystallinity is likely.[2] Poly(diethylsiloxane) fits this definition. Thermal analysis[3] shows a series of transitions that suggest a stable condis mesophase in the range of 200–290 K, and the presence of a high-temperature phase with some residual order up to the final transition to the isotropic liquid at about 310 K.

The multiple first-order transition behavior of poly(diethylsiloxane) (PDES) was first described by Lee et al.[4] in 1969 without interpretation. Later, in 1975, Beatty, Pochan, Karasz, and co-workers described the high-temperature phase in terms of "liquid crystalline" and "viscous crystalline" polymers.[5–9] The first suggestion that a condis phase of PDES exists in the temperature range of about 200–290 K was published in 1982.[1] At the same time Papkov et al.[10,11] proposed dimorporphism of the crystal and condis phase. The two pairs of dimorphs were called α_1, α_2 (crystals) and β_1, β_2 (condis crystals). The first calorimetry was already given by Beatty and Karasz.[6] Definitive calorimetry was produced by Lebedev et al.[12] Finally, an ATHAS review of all thermal analyses and calorimetry[3–5,10–13] that included also a link to the vibrational specrum led to the recommended thermodynamic parameters listed in Table I and produced tables of recommended heat capacity, enthalpy, entropy, and free enthalpy (Gibbs function).[14] Direct evidence for the motion in the condis crystals was found by using NMR line-width studies[8] and ^{13}C and ^{29}Si MAS CP solid-state NMR measurements.[13]

In this paper molecular mechanics calculations on the isolated molecular chain of PDES are presented, and the complicated phase behavior of PDES is rationalized.

Table I
Recommended Thermodynamic Values for Transitions in Poly(diethylsiloxane)[a]

ΔS_x, J/(K mol)	0.75	$\alpha_m \rightarrow$ melt
T_x, K	308.5	
ΔS_i, J/(K mol)	6.5	$\beta \rightarrow \alpha_m$
T_i, K	282.7	
ΔS_d, J/(K mol)	13.2	$\alpha \rightarrow \beta$
T_d, K	206.7	
ΔC_p, J/(K mol)	34.5	glass transition
T_g, K	135	

[a] All crystal transitions are extrapolated to 100% crystallinity and condis crystallinity, and the transitions are assumed to be close to equilibrium. The glass transition parameters refer to completely amorphous polymers (see ref 14). Enthalpies of transition can be calculated from $T\Delta S = \Delta H$.

Computations

All computations refer to isolated chains. The molecule is constructed from the repeating units $\mu \equiv [(SiEt_2)–O–]$, which also represents the most likely X-ray unit cell dimension, c, although multiples are possible. Six repeating units of the molecule, as shown in Figure 1, were chosen for computational purposes to minimize end effects. Bonds about which rotations are attempted are numbered. All thermodynamic quantities are reported in kJ/

† Present address: Shell Development Co. Westhollow Research Center, P.O. Box 1380, Houston, TX 77001.
‡ Present address: United Technologies Research Center, Silver Lane, East Hartford, CT 06108.
§ Present address: Department of Chemistry, The University of Tennessee, Knoxville, TN 37996-1600.

0024-9297/90/2223-0849$02.50/0

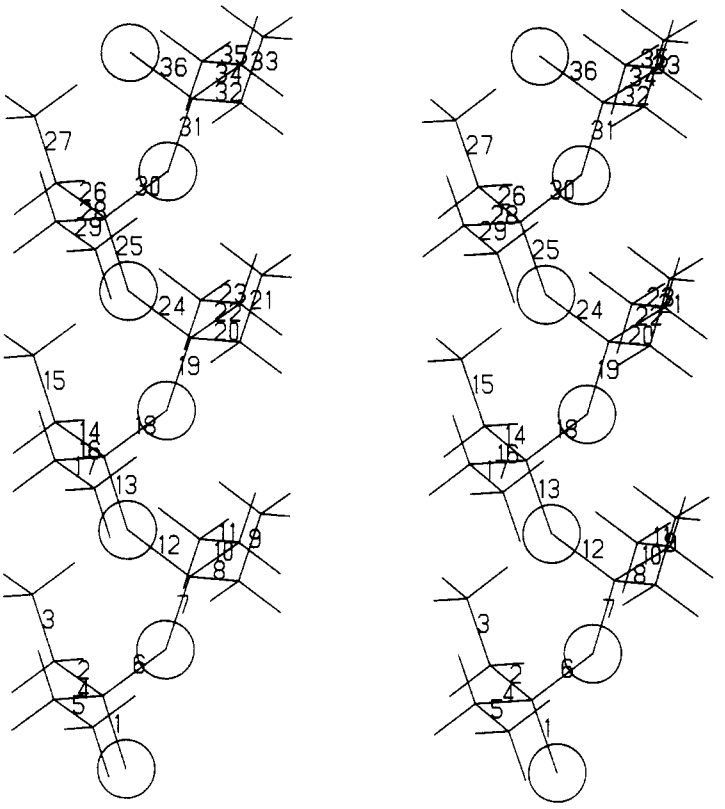

Figure 1. Stereographic projection of poly(diethylsiloxane). Rotations occur about number bonds. Bonds b = 2 and 8 are exactly trans, in sequences 1–2–3 and 7–8–9, respectively. Bonds b = 4 and 10 are exactly gauche, in sequences 1–4–5 and 7–10–11, respectively. All conformational angles are adjusted relative to the trans starting conformation, taken as 0°.

mol or J/(K mol) of the repeating unit μ. The notation δE defines the relative energy for the identified conformation and ΔE defines the energy change for a process. The unit $\mu_1\mu_2$ will be considered because it includes both distinct oxygen positions needed to establish a local chain symmetry and types of ethyl groups.

The torsion angles are defined in the stereo pair of Figure 1. For convenience all changes in the angles are measured relative to the flat backbone and to trans ethyl groups oriented in the sequence O–Si–Et as illustrated with bonds 2 and 8 ($\phi_2 = \phi_8 = 0°$). An example of gauche ethyl groups, rotated by −120°, is illustrated with bonds 4 and 10. The four distinct ethyl groups in the $\mu_1\mu_2$ polymer unit will be denoted in the order $\phi_2\phi_4\phi_8\phi_{10}$ by t, g^+, and g^-, where $\phi_b = 0° \pm 60°$ for t, $\phi_b = 120° \pm 60°$ for g^+, and $\phi_b = -120° \pm 60°$ for g^-. In the conformation illustrated, the principal axis bisects the two oxygens of the dimer and the overall conformation is tg^-tg^-. Three symmetry operations are possible: (1) C_2 + t, a 2-fold rotation about the principal axis (C_2) plus a translation by t = r(Si–O)[1 − cos θ], where $\theta = \theta$(Si–O–Si) is the angle about the oxygen atom, (2) σ_v + t, a reflection (σ_v) in the plane perpendicular to the average plane of the backbone plus t, and (3) σ_h, a reflection in the plane (h) containing the backbone. A translational repeat of nt, n = 0, 2, 4, ... or 1, 3, 5, ... is utilized to relate the units that are incorporated into a crystal. Asymmetric chains are also possible by mixing symmetries relating to one pair of ethyl groups. The study was conducted by assuming that all equivalent bonds along the polymer rotate in concert; i.e., adjustments to the torsional angles are grouped as follows: ϕ_{b+12n} where n = 0, 1, and 2 are set equal to yield the repeat units for each angle in the set of 12 independent torsional angles (b = 2, 3, 4, ..., 13) in the $\mu_1\mu_2$ unit. This assumption preserves local regularity assumed to occur in packing of the polymer.

The calculations were performed by allowing interactions between all atoms not bonded through a common atom (i.e. bond length and bond angles are kept constant except for θ) and the torsional changes. The atoms are grouped so that those directly bonded constitute a fragment. For rotations about each of the bonds indicated in Figure 1, the sum of the steric (U), electrostatic (Q), and torsional (T) energies

$$E = U + Q + T \tag{1}$$

are adjusted to minimize the total energy, E. Relative conformational energies

$$\delta E = E - E(\mathrm{fv_1fv_2}, 145°) \tag{2}$$

are reported, where $E(\mathrm{fv_1fv_2}, 145°)$ is chosen as the energy of the optimized flat conformation, $\mathrm{fv_1fv_2}$, defined below, at a Si–O–Si angle of θ = 145°.

The energy terms of eq 1 are obtained from a sum of two-body interactions between atoms i and j in different fragments.[15] The steric energy between atoms i and j is calculated with a 6–n potential (n = 14)

$$U_{ij}(s_{ij}) = [A_{ij}/\rho_{ij}^6][1/s_{ij}^6 - 6/(ns_{ij}^n)] \tag{3}$$

where $s_{ij} = r_{ij}/\rho_{ij}$ is the reduced distance with ρ_{ij} being the sum of van der Waals radii and $A_{ij} = -1.5\alpha_i\alpha_j I_i I_j/(I_i + I_j)$ is the London dispersion coefficient with atomic polarizabilities (α_i and α_j) and ionization potentials (I_i and I_j). Parameters used with this potential are defined elsewhere,[15] and α_{Si} = 0.002 00 nm^3, ρ_{Si} = 0.20 nm, and I_{Si} = 8.149 eV. The electrostatic energy between atoms i and j is calculated with the Coulomb potential

$$Q_{ij} = 138.93 q_i q_j / r_{ij} \text{ [kJ nm/(mol eu}^2\text{)]} \tag{4}$$

where q_i and q_j are the net atomic charges in electron units (eu). In this investigation we used the net charge

Table II
Conformations of Subunits μ_1 and μ_2 and Relative Energies of Poly(diethylsiloxane)[a]

μ_1						μ_2						δE,	type		
ϕ_2	ϕ_3	ϕ_4	ϕ_5	ϕ_6	ϕ_7	ϕ_8	ϕ_9	ϕ_{10}	ϕ_{11}	ϕ_{12}	ϕ_{13}	kJ/mol	$\mu_1\mu_2$	$\phi_2\phi_4\phi_8\phi_{10}$	g
Family I															
25	-1	-25	1	0	0	25	-1	-25	1	0	0	0.0	fv_1fv_2	tttt	1
113	-1	-15	-5	0	0	32	-4	-10	-2	0	0	0.9	fgt_1ftt_2	g^+ttt	2
113	-2	-8	-7	0	0	113	-2	-8	-7	0	0	0.7	fc_1fc_2	g^+tg^+t	2
22	-1	-27	2	2	-3	27	-2	-22	1	-2	3	0.0	v_1v_2	tttt	2
114	-1	-2	-1	-8	0	114	-1	-2	-1	-8	0	-0.2	c_1c_2	g^+tg^+t	2
Family II															
140	2	-7	7	0	0	114	-2	-144	-5	0	0	3.9	fgt_1fgg_2	$g^+tg^+g^-$	2
142	3	-142	-3	0	0	142	3	-142	-3	0	0	6.4	f_1f_2	$g^+g^-g^+g^-$	1
-148	-1	111	-4	-56	-12	-148	-1	111	-4	-56	-12	5.8	c_1c_2	$g^-g^+g^-g^+$	2
-151	-1	112	-3	-26	41	-112	3	151	1	26	-41	6.6	v_1v_2	$g^-g^+g^-g^+$	2

[a] The conformational angles, ϕ_b, are measured relative to the trans conformation shown in Figure 1. The energy δE and components are measured relative to the values for conformation fv_1fv_2 at θ(Si–O–Si) = 145°. Equivalent conformations are obtained by a mirror symmetry operation σ through the average plane of the backbone according to $\phi_i = -\phi_j$, where (i, j) = (2, 4), (3, 5), (8, 10), and (9, 11) for the ethyl groups and (6, 6) (7, 7), (12, 12), and (13, 13) for the backbone or by interchanging units $\mu_1\mu_2$.

$q_O = -0.50$, $q_{Si} = +0.40$, and $q_C = 0.05$ for the carbon atom bonded to silicon. These values were obtained from molecular orbital calculations.[16,17] The geometrical parameters are r(Si–O) = 0.1637 nm, r(C–H) = 0.110 nm, and r(Si–C) = 0.1867 nm. All angles except θ are tetrahedral. The torsional energy for each bond (b) is calculated with

$$T_b = (V/2)(1 - \cos 3\phi_b) \quad (5)$$

Values of the barrier to rotation, V, are 12.55 kJ/mol for C–C, 6.3 kJ/mol for Si–C, and 0.4 kJ/mol for Si–O.

The energy required to deform the θ(Si–O–Si) angle is small. Measurements in disiloxane suggest equilibrium values of 144.1° from electron diffraction,[18] of 155° from infrared spectroscopy at 20 K,[19] of 149 ± 2° in the gaseous and solid states,[20] and of 149.5° calculated quantum mechanically at the 3-21G level.[21] The barrier to linearization of Si–O–Si lies in the range of 1.34–5.86 kJ/mol.[19,20,21] The energy required to stretch bonds and alter angles is much larger than the linearization energy of the Si–O–Si angle. Consequently, all other bond lengths and angles were fixed. If a potential for the θ(Si–O–Si) deformation is included as a harmonic potential, the minimum shifts toward the assumed equilibrium value of θ_{eq} = 145° with

$$V(\theta) = 0.00478(\theta - 145°)^2 \text{ [kJ/(mol deg}^2\text{)]} \quad (6)$$

and reproduces the barrier of 5.86 kJ/mol at θ = 180°.

Calculations were performed at 10-deg increments of the θ(Si–O–Si) angle from 110° to 160° to develop a potential surface. The calculations were also repeated with all barriers to rotation taken as 12.55 kJ/mol to examine the effect of these parameters and rotational energy contributions to the minimum energy conformations. The conformations and the order of the states remain relatively unchanged on increasing the Si–C and Si–O rotational barriers. Sample calculations with a partitioning of the energy were, finally, performed to examine the importance of the Coulomb, steric, and torsional contributions. Steric effects keep the ethyl groups away from the bulk of the chain, and the 3-fold rotational barrier about Si–C directs them into trans and gauche orientations, leading to distinct families of conformations of minimum energy. Characteristic conformations appear independently of the electrostatic energies for the range of selected parameters. Overall, poly(diethylsiloxane) has much less rotational freedom about the backbone than poly(dimethylsiloxane) which has much less steric hindrance.[22]

Results

The systematic study resulted in the set of minimum energy conformations that are reported in Table II for θ(Si–O–Si) = 145° and is illustrated in Figures 2 and 3. These conformations are characterized as (1) flat conformations (f) in which the backbone angles vanish ($\theta_6 = \phi_7 = \phi_{12} = \theta_{13} = 0°$); (2) helices ($c_1c_2$ and corresponding mirror images of opposite handedness $\mathbf{c_1c_2}$) in which the backbone rotation angles are related by $\phi_6 = \phi_{12}$ and $\phi_7 = \theta_{13}$ and the ethyl group rotation angles by $\phi_b = \phi_b+6$ (b = 2, 3, 4, and 5); (3) vertical conformations (v_1v_2 and the mirror image $\mathbf{v_1v_2}$) with symmetry σ_v + t in which the backbone rotation angles are related by $\phi_6 = -\phi_{12}$ and $\phi_7 = -\phi_{13}$ and the ethyl group rotation angles by $\phi_2 = -\phi_{10}$, $\phi_4 = -\phi_8$, $\phi_3 = -\phi_{11}$, and $\phi_5 = -\phi_9$; and (4) asymmetric conformations with g^+ttt or $g^+tg^+g^-$ ethyl groups. Flat conformations that exhibit in addition the helical symmetry C_2 + t are labeled fc_1fc_2 and conformations that exhibit also the vertical symmetries σ_v + t and σ_h are labeled fv_1fv_2. The conformations fgt_1fgg_2 and fgt_1ftt_2 have mixed ethyl group conformations.

The energy, $\delta E + V(\theta)$, is illustrated as a function of the Si–O–Si angle in Figure 4. Addition of the bending potential energy $V(\theta)$ to δE shifts the minimum toward 145°. Two families of flat conformations are classified on the basis of Figure 4. Family I exhibits low-energy conformations in the region $\theta \approx$ 140–150° and family II exhibits in the region of $\theta \approx$ 120–130°. The potential surface is relatively flat, and the crystal packing energies will, in addition, modify the conformations, so we assume for the further discussion that the conformations at θ = 145°, described above, are representative for the description of the crystals. The ethyl groups in family I are oriented at $\phi_2 \approx 113°$ and $\phi_4 \approx -5°$ for fc_1fc_2 and c_1c_2 (g^+tg^+t conformations) and at $\phi_2 \approx 24°$, $\phi_4 \approx -26°$, $\phi_8 \approx 26°$, and $\phi_{10} \approx -24°$ for fv_1fv_2 and v_1v_2 (tttt conformation); and finally, if one of the ethyl groups is in the alternate conformation, then g^+ttt occurs. The ethyl groups in family II are oriented at $\phi_2 = -\phi_4 \approx 140°$ for f_1f_2 ($g^+g^-g^+g^-$ conformations); $\phi_2 \approx -150°$, $\phi_4 \approx 112°$ for c_1c_2 and v_1v_2; and in addition, $\phi_8 \approx -150°$ and $\phi_{10} \approx 112°$ for c_1c_2 and $\phi_8 \approx -112°$ and $\phi_{10} \approx 150°$ for v_1v_2 ($g^-g^+g^-g^+$ conformation); and finally, if one of the ethyl groups is in an alternate conformation, then $g^+tg^+g^-$ occurs.

The backbone is essentially flat in family I but exhibits an approximate 5/1 helix in family II for all Si–O–Si angles studied. Family I contains three distinct flat chain conformations and three distinct ethyl orientations, as is required to explain the NMR spectrum.[13] They are

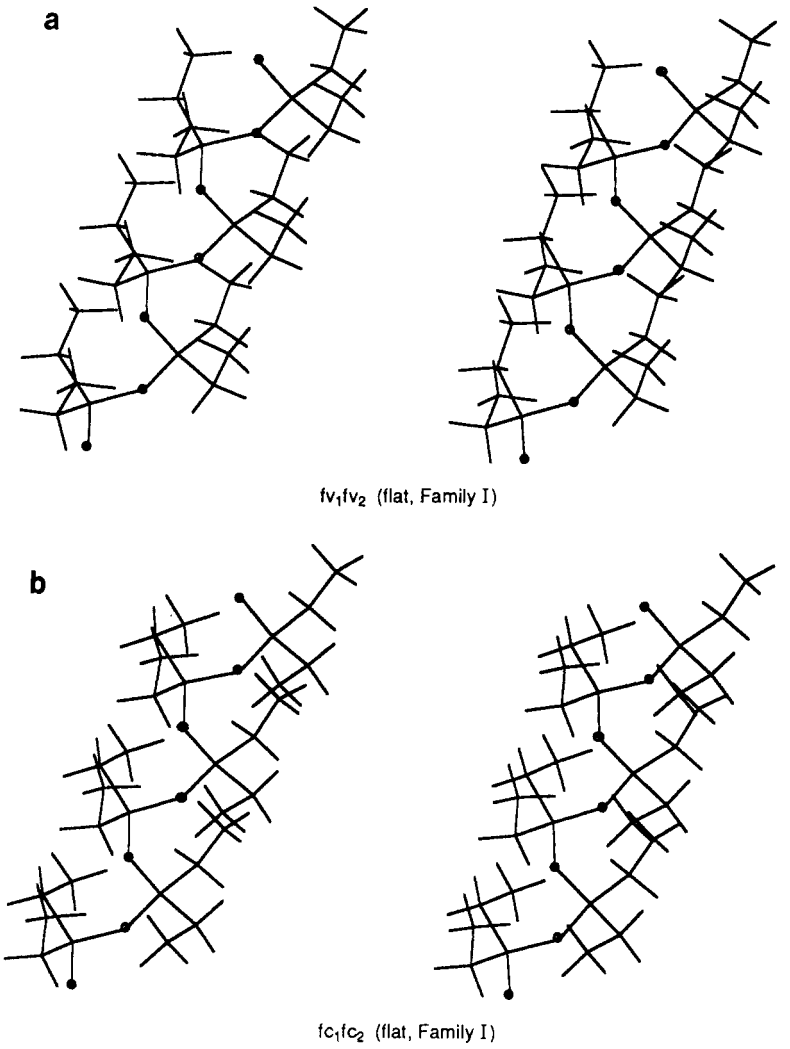

Figure 2. Stereographic projections of several trimer units: (a) fv_1fv_2 in family I and (b) fc_1fc_2 in family I, all at the θ(Si–O–Si) bond angle = 145°. For detailed descriptions see Table II.

energetically acceptable and conformationally fit the crystal structure. We assume thus that the flat conformations of family I make up the different α crystal structures.

The energy for concerted rotation of ethyl groups by changing ϕ_2 (or equivalently ϕ_8) in fv_1fv_2 and fc_1fc_2 and ϕ_4 (or equivalently ϕ_{10}) in fc_1fc_2, is shown in Figure 5. Family I conformation fv_1fv_2 is accessible by a rotation of ϕ_2 (and ϕ_8) in fc_1fc_2 from 113° toward 25° with an energy barrier of about 4 kJ per ethyl group. Conversely, conformation fc_1fc_2 is accessible by a rotation of ϕ_2 (and ϕ_8) in fv_1fv_2 from 25° to 113° with an energy change less than 10 kJ per ethyl group. Conformations in family I with ϕ_4 as g^- are not accessible by a rotation of only this type of ethyl group in fc_1fc_2, as seen by the large repulsive energy in the entire g^- region. However, cooperative motion of both ϕ_2 and ϕ_4 in fc_1fc_2 with ϕ_2 (or ϕ_8) increasing toward g^+ (142°) as ϕ_4 (or ϕ_{10}) decreases toward g^- (-142°) connects with conformation f_1f_2 in family II with an estimated barrier of 15–20 kJ/mol. These barriers suggest that mobility within and between families I and II connects the ethyl groups by successive changes in a process such as

$$\begin{array}{lcccccc} & tttt & \rightarrow & g^+ttt & \rightarrow & g^+tg^+t & \rightarrow & g^+tg^+g^- & \rightarrow & g^+g^-g^+g^- \\ \phi_2: & t \rightarrow g^+ & & & & & & & & \\ \phi_8: & & & t \rightarrow g^+ & & & & & & \\ \phi_4: & & & & & & & t \rightarrow g^- & & \\ \phi_{10}: & & & & & t \rightarrow g^- & & & & \end{array} \quad (7)$$

This mobility of the ethyl groups is used to rationalize the properties of the α and β crystal phases and to explain the $\alpha \rightarrow \beta$ condis phase transition. We speculate that conformations fc_1fc_2, fv_1fv_2, and fgt_1ftt_2 in family I may be responsible for the α_1 andd α_2 substructures and conformations f_1f_2 and fgt_1fgg_2 in family II for β_1 and β_2.

Molecular dynamics simulations must be used eventually to get average potential energy interactions and crystal structures. However, energy curves calculated by assuming that increased mobility of the ethyl groups depends on cooperative libration suggest an exchange between t and g^+ and g^- conformations within and between families I and II for the $\alpha \rightarrow \beta$ condis transition. Increased libration of the ethyl groups occurs as additional space in the solid becomes available.

The helical, vertical, and asymmetric conformations in which the backbones deviate substantially from the flat conformations may still occur in local regions of the chains. The effect of linking conformations together was studied by connecting them with transition regions: $...\mu_1\mu_2\mu_1(\phi_{18}\phi_{19})\mu_2'\mu_1'\mu_2'...$ at bonds 18 and 19. All combinations of the helical, bent, and the mirror images of the segments of family I of the polymer were thus joined. Values of the transition torsional angles ϕ_{18} and ϕ_{19} were selected from the approaching sequence $\mu_1\mu_2\mu_1$ and from the leaving sequence $\mu_2'\mu_1'\mu_2'$. The energy at the junction, measured as the difference between the calculated value for the hexamer and that of the separate trimers of the sequence entering and leaving this region, remained

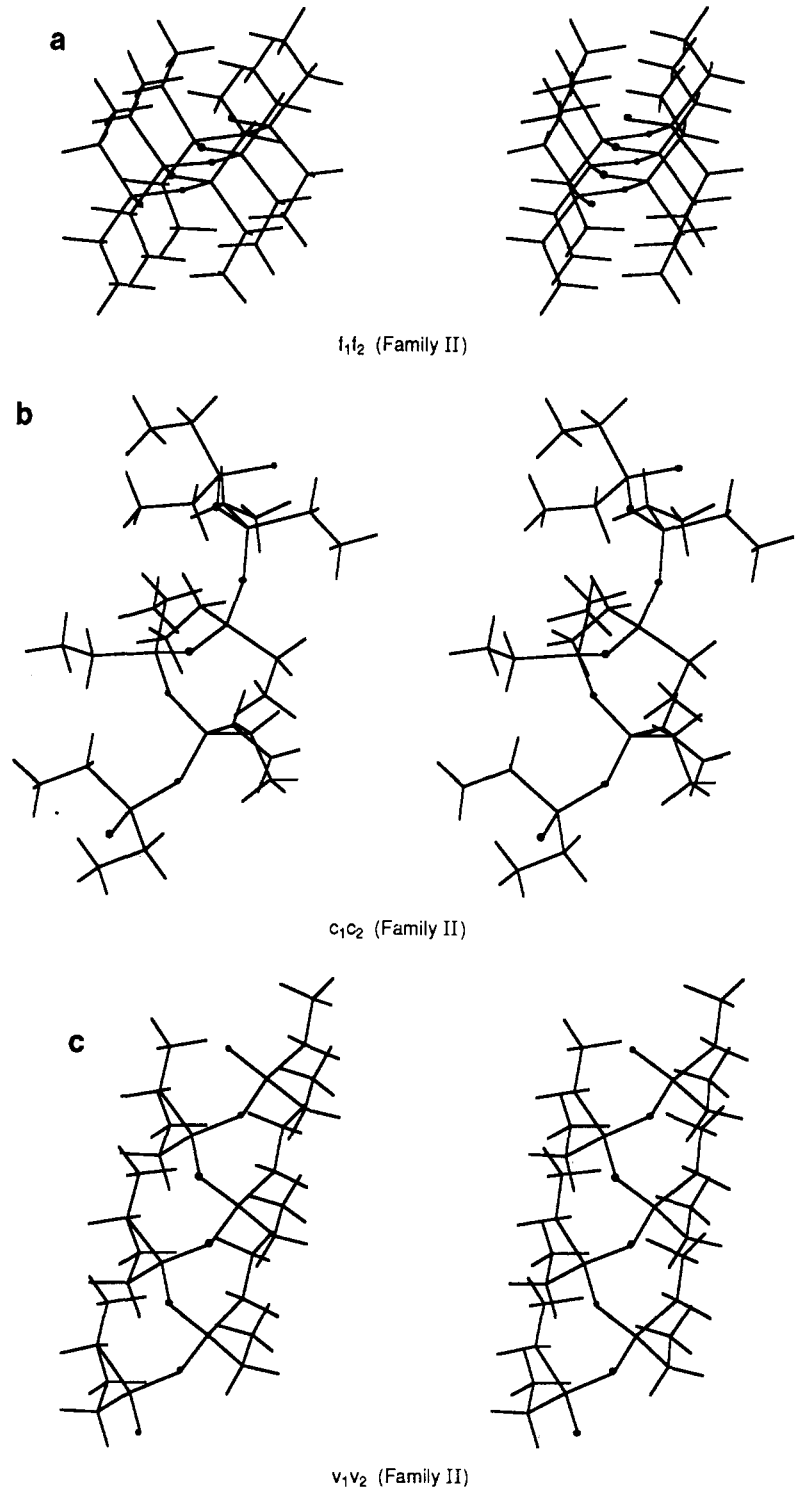

Figure 3. Stereographic projections of several trimer units: (a) f_1f_2 in family II, (b) c_1c_2 (5/1 helix) in family II, and (c) v_1v_2, in family II, all at the θ(Si–O–Si) bond angle = 145°. For detailed descriptions see Table II.

below 15 kJ/mol for 90% of the examples studied. Several sequences with very favorable transition energies are shown in Figure 6. Especially important are the possibilities to connect helical and bent regions. For example, c_2c_1 links to v_2v_1 with 2.1 kJ/mol and returns to the c_2c_1 with 3.2 kJ/mol. Alternatively, c_2c_1 links to v_2v_1 with 1.1 kJ/mol, to $\mathbf{c_2c_1}$ with 3.2 kJ/mol, and to v_2v_1 with 1.1 kJ/mol and returns to the c_2c_1 with 3.2 kJ/mol, thus completing the cycle. Other combinations of cycles are possible. The curvature of the bent conformation is sufficiently large so that many repeat units can be accommodated locally. These transition regions permit the possibility of local regions of flat and helical conformations and may be used to explain conformations in the melt.

To judge the shape of the chains better, the excluded volume and surface area was evaluated and is shown in Figure 7. Conformations fv_1v_2, fgt_1ftt_2, and fc_1c_2, in family I and fgt_1fgg_2, f_1f_2, and c_1c_2 in family II illustrate the distinguishing features.[23] The cross sections of flat conformations in family I are rectangular, despite the trans or gauche ethyl groups. The volume and surface area and surface irregularity increases with the number of gauche ethyl groups. Family II is larger than I by 5%. The c_1c_2 5/1 helix exhibits the most irregular surface.

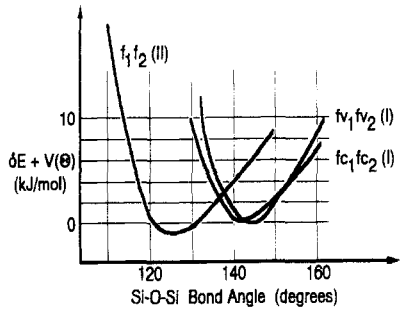

Figure 4. Potential energy $\delta E + V(\theta)$. Dependence of the flat conformations on the θ(Si–O–Si) bond angle.

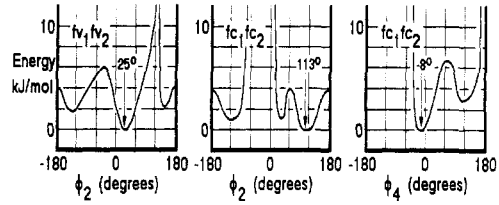

Figure 5. Energy for concerted rotation of pairs of ethyl groups required to connect fc_1fc_2 to fv_1f_2 in family I through ϕ_2 and fc_1fc_2 in family II through ϕ_4.

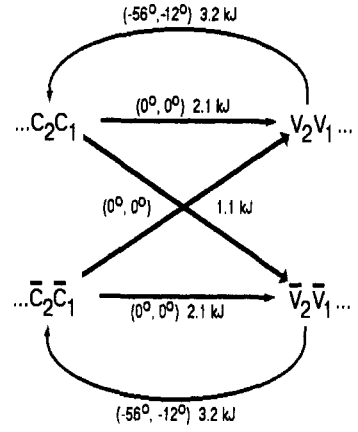

Figure 6. Transitions regions connecting c_2c_1, v_2v_1, and mirror images at the junction defined by (ϕ_{18}, ϕ_{19}) and δE.

One may expect that family I conformations will pack more readily to form a monoclinic crystal structure than those of family II. This observation supports the loosening up of the chains in our assignment of conformations that participate in each of the phases: α, β, α_m, and melt.

The major result of the computation displayed in Table II is the recognition of the importance of the steric hindrance to determine the overall chain conformation. It is well established that C, N, and O atoms in the backbone chain govern the overall conformation by requiring torsional (rotational isomeric) states close to trans or gauche isomers. This overriding intrinsic hindrance to rotation has led to the well-known principles for prediction of the conformation of macromolecular motifs in helices, developed by Natta and co-workers.[24] These do not apply to the Si–O backbone. Similar observations were made earlier for the crystals of polyphosphates.[25] The source of the various conformations of minimum energy in poly(diethylsiloxane) is inter- and intramolecular steric hindrance and intrinsic hindrance to rotation of the side chains only, not the main chain. Packing into a crystal gives the final reason for the selection of specific combinations of ethyl group conformations.

The limit of the present computation lies with the restriction to the isolated chain. For C, N, and O backbone molecules it has often been sufficient to make such isolated chain calculations because of the overriding importance of the intrinsic hindrance to rotation of the backbone. In the present case the large intramolecular steric hindrance of the ethyl group permits a similar simplification and contributes to an apparent chain stiffness when the ethyl groups act cooperatively to avoid bad contacts. In the case of poly(dimethylsiloxane), in contrast, the methyl groups are relatively free to rotate and the polymer remains flexible, as expected from the ease of rotation about the Si–O bonds.

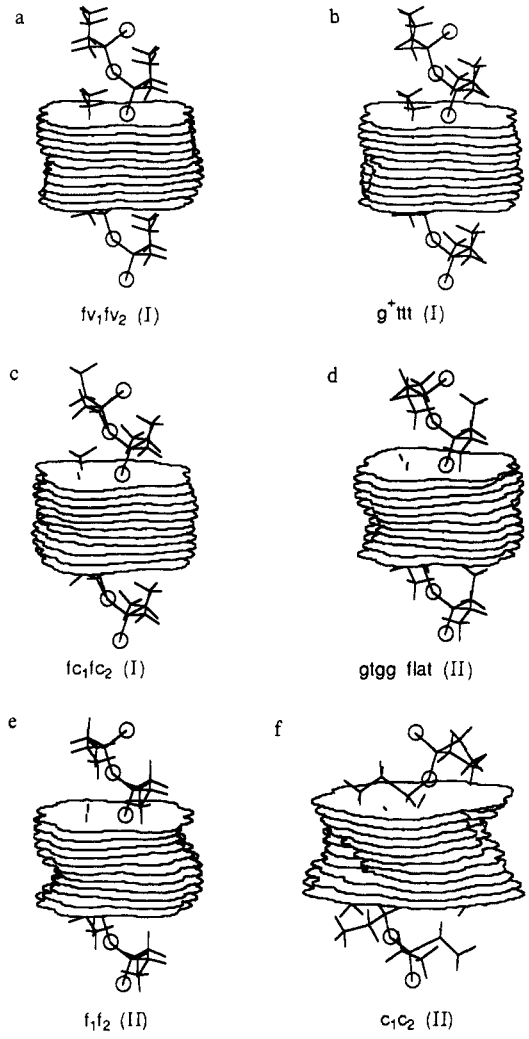

Figure 7. Excluded volumes and surfaces of flat and 5/1 helical conformations over two repeat units for conformations (a) tttt, (b) g^+ttt, (c) g^+tg^+t, (d) $g^+tg^+g^-$, (e) $g^+g^-g^+g^-$ and (f) c_1c_2 (5/1 helix).

The computed conformations are expected to be changed somewhat by including bond-bending and -stretching terms in the computation, but recognition of the weak potential dependence of the Si–O–Si angle in the calculation yields characteristic families of conformations and types of ethyl groups. Also, it is expected that intermolecular steric terms in a crystal computation would improve the fit with the experiment. The ultimate, as always, being a multiple-chain molecular dynamics computer simulation. It is hoped that funds can be found to carry out such simulation in the near future, mainly to solve the remaining problems of the high-temperature mesophase α_m.

Discussion of Crystals, Condis Crystals, and Melt

a. Conformation in the α Crystal. The five flat conformations fv_1fv_2, fgt_1ftt_2, and fc_1fc_2 of family I satisfy

Table III
Physical Characteristics of the Conformations at $\theta = 145°$

conf	c, nm	S, nm^2	V, nm^3
	Family I		
fv_1fv_2	0.2550	0.9683	0.1954
fgt_1ftt_2	0.2550	0.9949	0.1997
fc_1fc_2	0.2550	1.0192	0.2054
v_1v_2	0.2549	0.9681	0.1955
c_1c_2	0.2546	1.0355	0.2071
	Family II		
fgt_1fgg_2	0.2550	1.0501	0.2100
f_1f_2	0.2550	1.0755	0.2116
c_1c_2	0.2281	1.0755	0.2105
v_1v_2	0.2522	1.1161	0.2121

the requirements of straight chain and low energy and fit into the crystal with minimum volume (see Figure 7a–c). We assume localized regions of these conformations to constitute the crystalline α phase, with possibly α_1 and α_2 as substructures. In support of this assignment it was found that the solid-state ^{13}C NMR (MAS-CP) detects at least three sets of resonances for the CH_3 and CH_2 carbons at low temperature; i.e., the chain must be made up of at least three different conformational isomers.[13] Checking family I in Table II there are, indeed, only three ethyl rotational angles (ϕ_2, ϕ_4, ϕ_8, and ϕ_{10}) that govern these conformations [±113°, ±(8–15)°, ±(25–32)°]. In contrast, ^{29}Si NMR shows at 190 K a single, somewhat broader peak.[13] Checking Table II for bond rotations that govern the ^{29}Si chemical shift, namely ϕ_6 and ϕ_7 with ϕ_{12}, and ϕ_{13}, one finds that they vanish for the flat conformations. Even if conformations with slightly helical chains should occur locally, the changes in backbone rotation angles are small.

The polymorphism reported at low temperature by X-ray diffraction[3,5,9–11] can easily be explained by the multitude of packing of chains that is possible with these different conformations. The X-ray diffraction patterns of the α_1 and β_1 polymorphs, proposed to be monoclinic and tetragonal, respectively, show only minor differences, in line with the minor changes in the conformations. The solid-state NMR of ^{13}C and ^{29}Si shows differences in the locations of the resonance signals, but not in their number, so that one may assume that mixed conformations exist in both polymorphs.

b. Transformation to the Condis State (α to β Transition). The transformation from the crystal to the condis state at T_d shows the largest transitional change in entropy (see Table I). The X-ray crystal diffraction pattern changes relatively little and the four major diffraction peaks remain, but many of the minor peaks disappear.[11] The chain extension remains the same, but a 6% increase in volume was observed. A similar change in molecular volume occurs on going from family I conformations to family II conformations. This can be seen from the data in Table III that were calculated from steric contours (see Figure 7).[23] Listed are the repeat distance, c, the surface area, S, and the volume for the [($SiEt_2$)–O–] unit. We postulate thus that the disordering transition take place by going from conformations of family I to family II. This phase transition can be accomplished by cooperative moving of the ethyl groups along paths connecting the conformations (see eq 7). At the same time, the larger volume of the family II conformations may also permit continuing cooperative interchanges between the different ethyl group conformations.

Experiments responsive to motion document the high mobility in the side chains of PDES.[1] Proton NMR[8] shows at T_d a jump in the crystalline spin–spin relaxation time to the value of the amorphous portion in semicrystalline samples. The ^{13}C CP-MAS spectrum shows a coalescence of the six lines to two lines, one for CH_3 and one for CH_2, while the ^{29}Si spectrum shows little change in line shape.[13] The chemical shift anisotropy of ^{13}C becomes narrower and that of ^{29}Si stays the same, indicative of less backbone than side-chain motion in the NMR time scale.[13]

All these experimental indications have been used to support the assignment of the intermediate crystal phase as a condis crystal with increased side-chain mobility.[12] The present calculations suggest that motion of a single ethyl group results in energy changes which depend on the orientation of other ethyl groups. Cooperative libration are possible with less than 12 kJ/mol increase in potential energy for rotations about ϕ_2 from 20° toward 120° for fv_1fv_2 and from 20° toward 280° (−80°) for fc_1fc_2 and for rotation about ϕ_4 from −20° toward 170° for fc_1fc_2. The proposed model calls for such large amplitude librations of the side chains, erasing the differences between the conformational isomers, coupled with small readjustments of the essentially flat backbone. The former accounts for the coalescence of the ^{13}C signal and the step in the ^1H spin–spin relaxation time, the latter for the shift in ^{29}Si signal without change in CSA. The flat conformations in families I and II with t, g^+, and g^- type ethyl groups are sufficient to give a plausible explanation for all experimental data.

c. The High-Temperature Mesophase Melt. The transitions from the condis state to the α_m phase was described originally as a "liquid crystalline" or "viscous crystalline" polymer of partial crystallinity.[5–9] Indeed, minor mechanical disturbances change the phase behavior. Although no exact conclusions can be drawn from the present calculations, it is obvious, and in accord with the limited experimental evidence, that multiple possibilities of t, g^+, and g^- conformations are possible in this phase with maximum ethyl mobility. The total entropy of transition between the β phase and the melt is about 7.3 J/(K mol), of which 6.5 J/(mol K) is attributed to the $\beta \rightarrow \alpha_m$ transition. This entropy could account for conformational freedom about one bond, when estimated from the average established for many linear macromolecules.[1,26]

We speculate that this additional mobility is introduced in stages. Initially, at T_i, sequences of relatively rigid backbone with conformations as listed in Table II remain. These sequences represent mesogens along the chain and may have proper length to stabilize a liquid crystalline α_m phase. These mesogens are, however, neither permanent nor make up the total chain. The α_m phase is thus to be looked upon as a lyotropic liquid crystal where parts of the same molecule provide mesophase and solvent in a microphase-separated structure (partial mesophase crystallinity). As the temperature increases, the number of breaks in the linearity of the chain increases and the mesophase crystallinity decreases, leading ultimately to the isotropic melt. This speculation could account for the rather broad transition. It could also explain the enhancement of the α_m phase on deformation. Ultimately, it could also account for the fact that molten PDES can be quenched to an isotropic glass, something not possible with most liquid crystalline polymers which usually form glasses with liquid crystalline structure (LC glasses) and display an almost reversible disordering transition.[1] Also, the variable and occasional large supercooling of the melt to the α_m and condis phase could

be accounted for by assuming a rather sluggish attainment of parallel (flat) chain conformations. In the melt, there is a breakdown of the long-range order. Stable helical and bent conformations with backbone bond rotation angles $-56° < \phi_b < -12°$ and $-26° < \phi_b < 41°$ are possible as well as local conformations that are linked together as illustrated in Figure 6, as an example.

d. Energetics and Entropies of the Transition at T_d. To rationalize the transition from the crystal to the mesophases, we assume a change from a fixed, mixed crystal conformation to the melt mainly through ethyl group rotation. The entropy gained from this rotation of the ethyl groups may be estimated by starting from the energy of a restricted rotor

$$E_n = (h/2\pi)^2[n^2/(IL^2)] \tag{8}$$

Next one can calculate the partition function

$$Z = \sum_n e^{-E_n/(RT)} \tag{9}$$

and entropy

$$S = R \ln Z \tag{10}$$

where $I = 0.3546$ amu $(\text{nm})^2$ is the moment of inertia for an ethyl group, $L = \phi_c/180°$, with ϕ_c defining the cutoff angle of the restricted rotation, and h and k being Planck's and Boltzmann's constant. The change in entropy is $\Delta S = 24.8$ J/(mol K) if two ethyl groups change from a completely restricted state to free rotation. With the cutoff angles $\phi_c(\alpha) = 15°$, $\phi_c(\beta) = 43°$, $\phi_c(\alpha_m) = 68°$, and $\phi_c(\text{melt}) = 72°$, the following entropies can be calculated: $\Delta S(\alpha \rightarrow \beta) = 13.6$ J/(K mol), $\Delta S(\beta \rightarrow \alpha_m) = 6.4$ J/(K mol), and $\Delta S(\alpha_m \rightarrow \text{melt}) = 0.8$ J/(K mol), for two ethyl groups. This calculation should only serve to illustrate that the present model can rationalize the thermal properties by assuming motion of the side groups only, as was proposed earlier.[1]

Conclusions

Conformations of PDES computed are used to rationalize the various observed phases. Crystal phase $\alpha(\alpha_1$ and $\alpha_2)$ may be explained by several conformations (and mirror images) of family I with flat backbones and ethyl groups in the all-trans or with up to two gauche conformations (see Figures 2a,b and 7a–c). Mesophase $\beta(\beta_1$ and $\beta_2)$ may be explained by conformations of the family II with three and four gauche-type ethyl groups (see Figures 3a and 7e,f) and an increase in volume that permits large amplitude ethyl group librations. Mesophase α_m may be characterized by maximum mobility of the ethyl groups and conformations of both families I and II, which readily exchange conformations but retain a certain temperature-dependent fraction of flat sequences that act as mesogens and cause a liquid crystal-like phase. Finally, the melt is similar to the α_m phase and includes all conformations that are not flat such as the 5/1 helices, bent conformations (see Figure 3b,c), and short segments of linked conformations. None of the flat sequences is long enough and of sufficient concentration to give a liquid crystalline appearance. As the trans ethyl groups get replaced by gauche ethyl groups, the volume and surface area increases and the surface becomes more irregular, which suggests a decrease in packing ability and gives a rationalization for the phase changes. Conformations tttt, g^+ttt, and g^+tg^+t appear compatible with α phase and $g^+tg^+g^-$ and $g^+g^-g^+g^-$ with the β phase at a 5% larger volume and greater ethyl group libration. This model can be brought into agreement with the experimental data.

Acknowledgment. This work was supported by the NSF, Polymers Program, Grant DMR 8818412. Early work on the silicone polymers of J.P.W. was supported by the donors of the Petroleum Research Fund, administered by the American Chemical Society. We also express appreciation to Rensselaer Polytechnic Institute for a generous grant of computer time.

References and Notes

(1) Wunderlich, B.; Grebowicz, J. *Adv. Polym. Sci.* **1984**, *60/61*, 1. See also partial preprints: In Miller, B., Ed. *Thermal Analysis*; Wiley-Heyden: Chichester, 1982; Vol. II, p 1084.

(2) Wunderlich, B.; Möller, M.; Grebowicz, J.; Bauer, H. *Adv. Polym. Sci.* **1988**, *87*, 1.

(3) Wiedemann, H. G.; Grebowicz, J.; Wesson, J.; Wunderlich, B. *Proc. 12th Natas Conf.* **1983**, 295. Wiedemann, H. G.; Wesson, J.; Wunderlich, B. *Mol. Cryst. Liq. Cryst.* **1988**, *155*, 469. See also: Wesson, J. P. Thesis, **1988**, Dept. of Chem. Rensselaer Polytechnic Institute, Troy, NY.

(4) Lee, C. L.; Johannson, O. K.; Flannigham; O. L.; Hahn, P. *Polym. Prepr.* **1969**, *10*(2), 1311, 1319.

(5) Beatty, C. L.; Pochan, J. M.; Froix, M. F.; Hinman, D. D. *Macromolecules* **1975**, *8*, 547.

(6) Beatty, C. L.; Karasz, F. E. *J. Polym. Sci., Polym. Phys. Ed.* **1975**, *13*, 971.

(7) Pochan. J. M.; Beatty, C. L.; Hinman, D. D. *J. Polym. Sci., Polym. Phys. Ed.* **1975**, *13*, 977.

(8) Froix, M. F.; Beatty, C. L.; Pochan, J. M., Hinman, D. D. *J. Polym. Sci., Polym. Phys. Ed.* **1975**, *13*, 1269.

(9) Pochan, J. M.; Hinman, D. D.; Froix, M. F. *Macromolecules* **1976**, *9*, 611.

(10) Papkov, V. S.; Godovsky, Y. K.; Svistunov, V. S.; Litvinov, V. M.; Zhadanov, A. A. *J. Polymer Sci., Polym. Chem. Ed.* **1984**, *22*, 3617.

(11) Tsvankin, D. Y.; Papkov, V. S.; Zhukov, V. P.; Godovsky, Y. K.; Svistunov, V. S.; Zhadanov, A. A. *J. Polym. Sci., Polym. Chem. Ed.* **1985**, *23*, 1043.

(12) Lebedev, B. V.; Kulagina, T. G.; Svistunov, V. S. Papkov, V. S.; Zhadanov, A. A. *Polym. Sci. USSR (Engl. Transl.* **1984**, *12*, 2773 (*Vysokomol. Soedin., Ser. A.* **1984**, *12*, 2476); see also Kulagina, T. G.; Lebedev, B. V. *Termodin. Org. Soedin.* **1982**, 18.

(13) Kögler, G.; Loufakis, K.; Möller, M. In *Integration of Fundamental Polymer Science and Technology III*, Lemstra, P. J., Kleinjiens, L. A., Eds.; Elsevier: London, 1989; Kögler, G.; Hasenhindl, A.; Möller, M. *Macromolecules* **1989**, *22*, 4190.

(14) Varma, M.; Wesson, J.; Wunderlich, B. *J. Therm. Analysis* **1989**, in press.

(15) Miller, K. J.; Brodzinsky, R.; Hall, S. *Biopolymers* **1980**, *19*, 2091.

(16) See, for example: Bingham, R. C.; Dewar, M. J. S.; Lo, D. H. *J. Am. Chem. Soc.* **1975**, *97*, 1285.

(17) Miller, K. J.; Pycior, J. F.; Moschner, K. F. *QCPE Bull.* **1981**, *1*, 67.

(18) Almenningen, A.; Bastiansen, O.; Ewing, V.; Hedberg, K.; Traettberg, M. *Acta Chim. Scand.* **1963**, *17*, 2455.

(19) Lord, R. C.; Robinson, D. W.; Schumb, N. C. *J. Am. Chem. Soc.* **1957**, *78*, 1327.

(20) Durig, J. R.; Flanagen, M. J.; Kalasinsky, V. F. *J. Chem. Phys.* **1977**, *66*, 2775.

(21) Grigoras, S.; Lane, T. H. *J. Comput. Chem.* **1987**, *8*, 84.

(22) Bruckner, S.; Malpezzi, L. *Makromol. Chem.* **1982**, *183*, 2033.

(23) Miller, K. J.; Kowalczyk, P.; Segmuller, W.; Walker, G. *J. Comput. Chem.* **1983**, *4*, 366.

(24) Natta, G.; Corradini, P.; Ganis, P. *J. Polym. Sci.* **1960**, *58*, 1191.

(25) Wunderlich, B. *Macromolecular Physics*; Academic Press: New York, 1973; Vol. 1.

(26) Wunderlich, B. *Macromolecular Physics*; Academic Press: New York, 1980; Vol. 3.